Egyptian Journal of Cell and Tissue Research
Print ISSN: 2812-5436 / Online ISSN: 2812-5444

The Possible Protective Effect of Atorvastatin on Azithromycin-Induced Cardiotoxicity in Adult Male Albino Rat: Light &Electron Microscopic Study

[1]Fatma Elzahraa Mohamed Abdellatif, [1]Azza Saleh Embaby, [2]Samar Gamal Sherbini & [1]Eman Mohammed Abdel-Hameed.

[1]Medical Histology & Cell Biology Department, Faculty of Medicine, Beni-Suef University
[2]Medical Histology & Cell Biology Department, Faculty of Medicine, Nahda University, Egypt

Abstract:

Background: With its antiviral and immunomodulatory actions, Azithromycin has been used in the protocol for treating COVID-19, either in conjunction with Hydroxychloroquine or on its own more recently. Myocardial apoptosis, oxidative stress and inflammation were all seen in rat models after Azithromycin treatment. A synthetic statin called atorvastatin has antioxidant and antiapoptotic properties that help reduce the damage caused by myocardial ischemia. The purpose of this research was to see whether Atorvastatin may mitigate the cardiotoxic effects of Azithromycin. **Aim of the work:** This study was performed to investigate histologically the possible protective effect of Atorvastatin on Azithromycin-induced cardiotoxicity in adult male albino rats. **Materials and Methods:** A total of 40 adult male albino rats were randomly split into four groups of ten animals each and treated with either a placebo, Azithromycin, Atorvastatin, or both. For two weeks, an intragastric tube delivered 30 milligrams of azithromycin per kilogram of body weight and 2 milligrams of atorvastatin. Rats were sacrified twenty-four hours after the final treatment, then their hearts were removed, and apical portions were processed for examination using light and electron microscopes followed by statistical testing. **Results**: Cardiac myocytes in the azithromycin group had fewer cross striations, an increase in inflammatory cell infiltration, a greater deposition of collagen fibers, localized degeneration of myofibers, disruption of sarcomeres, mitochondrial damage, and nuclear pyknosis. The atorvastatin and azithromycin-treated group saw these improvements first.

Conclusion: Light and electron microscopy results demonstrated that the Atorvastatin group had restored cardiac muscle fibers.

Keywords: Cardiac muscle, Azithromycin, Atorvastatin, Electron microscope.

1. Introduction:

Among the macrolide class of antibiotics, azithromycin (Zithromax) is one of the most popular choices. The FDA has given its approval for use against both pulmonary and STD infections (1). Azithromycin's antiviral action and immunomodulatory effects, either in combination with Hydroxychloroquine or alone, are two of the many reasons it may be useful in treating COVID-19 infection (2).

By enhancing the body's natural defenses against viruses, it reduces viral entrance into cells (3). This happens when genes involved in viral recognition and the synthesis of type I and III interferons (particularly interferon- and -) are turned up (4).

Those with preexisting cardiac conditions are more vulnerable because of the increased risk of QT prolongation caused by azithromycin. Researchers found that Azithromycin induced oxidative stress, inflammation, and apoptosis in rat heart muscle (5, 6).

Treatment of hypercholesterolemia and atherosclerotic disease with statins has become commonly used (7). By creating reactive oxygen species, they may inhibit mitochondrial dysfunction from worsening with hypertrophy or cardiac failure (ROS) (8).

Atorvastatin, an inhibitor of the enzyme hydroxy-methyl glutaryl-coenzyme A (HMG-CoA) reductase, has a number of beneficial effects on the body, including anti-inflammatory activity, reduced oxidative stress, enhanced endothelial function, increased angiogenesis, and decreased myocardial hypertrophy and remodeling (9,10).

2. Materials and Methods:

Drugs:

Azithromycin (Zithromax): It was purchased as a hard gelatin capsule each contains 250 mg from Pfizer company-Germany.

Atorvastatin (Lipitor): It was purchased as film coated tablets each contains 20 mg from Pfizer company-Germany.

Animals:

This research used 40 adult male albino rats 10-12 weeks old, weighing (200-250 gram) from the animal house at the Faculty of Pharmacy, Nahda University. Food and water were provided on an as-needed basis,

and they were housed in wire mesh cages in a well-ventilated room with regular access to both. To begin, 40 rats were allocated randomly among four groups. All medicines, including azithromycin and atorvastatin, were administered by intra-gastric tube after being dissolved in distilled water.

All experiments were conducted in accordance with Beni-Suef University's animal care and experimentation protocols at 13\6\2021 with Approval number (012-164).

Experimental design

The animals were divided into the following groups:

Group I (Control group, 10 rats):

Received distilled water 1 ml/100 g/day orally by gastric gavage for two weeks (11).

Group II (Azithromycin group, 10 rats):

Received Azithromycin 30 mg/kg/day orally by gastric gavage for two weeks (11). Rats weighing (200-250 gram) received 2ml from 30mg Azithromycin dissolved in 80ml saline.

Group III (Atorvastatin group, 10 rats):

Received Atorvastatin 2 mg/kg/day orally by gastric gavage for two weeks (12). Rats weighing (200-250 gram) received 2ml from 2mg Atorvastatin dissolved in 10ml saline.

Group IV (Combined Azithromycin and Atorvastatin group, 10 rats):

The rats received Azithromycin 30mg/kg/day orally via gastric gavage then after 1hour they received Atorvastatin 2mg/kg/day orally via gastric gavage for two weeks (12).

Experimental procedure

The animals were sacrificed after 2 weeks by anesthetic overdose of sodium pentobarbitone (200 mg/kg IP). Hearts were obtained by performing a ventral midline incision, exposure, and dissection. Then Heart specimens were fixed in 10% formol saline for 24 hours and processed for histological, ultrastructural, and morphometric studies.

Histological Study:

The following staining methods were applied on paraffin sections:

1. Hematoxylin and Eosin (H&E) (13).
2. Mallory's Trichrome Stain (14).
3. Tests using an electron microscope (transmission electron microscopy):

Small specimens from the left ventricle were fixed in 2-3 percent Glutaraldehyde, placed in the refrigerator overnight, processed, and post-fixed in osmium tetroxide in preparation for semithin and ultrathin sections. To determine which places would be best for creating ultrathin sections for the electron microscope, semithin sections were prepared, stained with toluidine blue dye, analyzed, and photographed. Ultrathin slices were cut, stained with uranyl acetate and lead citrate, and examined with a JEOL (JEM- 100cx)

transmission electron microscope at the Faculty of Agriculture at Cairo University (15).

II. Morphometric Study:

Area % of collagen stained with Mallory's trichrome was measured in all four groups using an image analyzer computer system with Leica Qwin 500 software at Beni-Suef University's Faculty of Veterinary Medicine (Cambridge, England). Ten randomly selected, non-overlapping nominated fields were evaluated at a magnification of 400 for each region.

III. Statistical Analysis (16)

Using SPSS version 25, we performed an analysis of variance (ANOVA) on the morphometric data, and then a post hoc Tukey test to compare the groups. If the P-value for the differences was less than 0.05, it was determined to be statistically significant.

3. Results:

1. Hematoxylin & Eosin-stained sections (Fig.1)

Sections of the hearts of control rats **(group I)** revealed branched cardiac cells with transverse striations and nuclei in the centers. Between the muscle fibers and the blood vessels that run alongside them is a thin layer of connective tissue called endomysium. This endomysium contains the rounded nuclei of fibroblasts. A significant number of muscle fibers were destroyed and the intercellular gaps became much more wider, as shown in the sections from **(group II)**. We observed some infiltration of inflammatory cells and constriction of blood vessels. Some myocytes possessed wavy, corrugated shapes, while others had developed foci of degeneration. Their nuclei were thick and pyknotic, and the sarcoplasm had become pale, disorganized, and devoid of transverse striations. **(Group III)** sections showed cardiac myocytes, which make up the heart's muscle cells, to be cylindrical in form with many branches and anastomoses. They have an oval, vesicular, acidophilic nucleus in the center of their sarcoplasm. When looking at myocytes, we saw that they had narrow endomysium gaps. At the endomysium's perimeter, fibroblasts with flat nuclei were seen around myocytes. Significant improvement has been made in analyzing sections of **(group IV)** cardiac muscle fibers. There were no areas of muscle breakdown, corrugation, or inflammatory cell infiltration. Myocytes appeared branched with narrow intercellular spaces. Sarcoplasm was deeply acidophilic and transversely striated. While some nuclei seemed typical, others were noticeably smaller. Capillaries were also shown to be dilated and swollen.

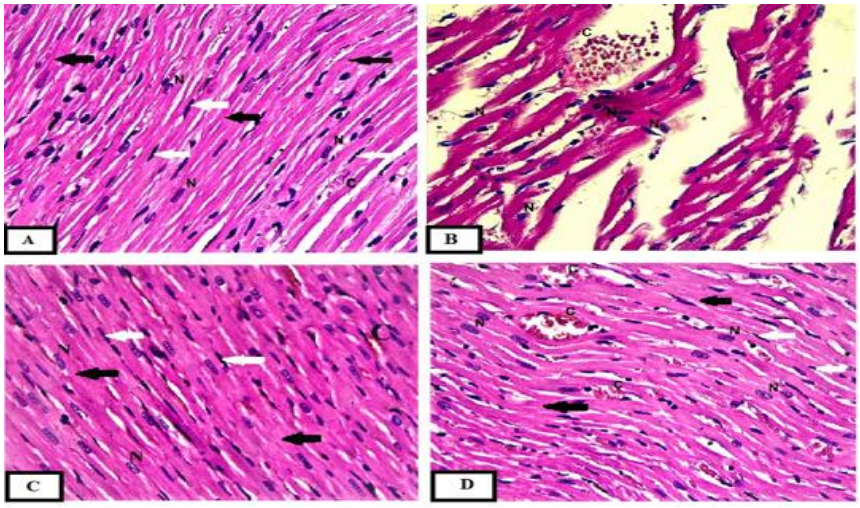

2. Mallory'strichrome stained sections (Fig. 2):

The collagen fibers accumulation around the capillaries and among the muscle fibers in the left ventricle of **(group I)** was low as shown in Mallory's trichrome stained sections. The sections of **(group II)** showed increased collagen fibers deposition among muscle fibers and around blood capillaries with obvious widening of intercellular spaces. Among muscle fibers and blood capillaries in **(group III)**, sections revealed just a few collagen fibers. Collagen fiber deposition among muscle fibers and surrounding blood capillaries was mild to moderate in **(Group IV)**.

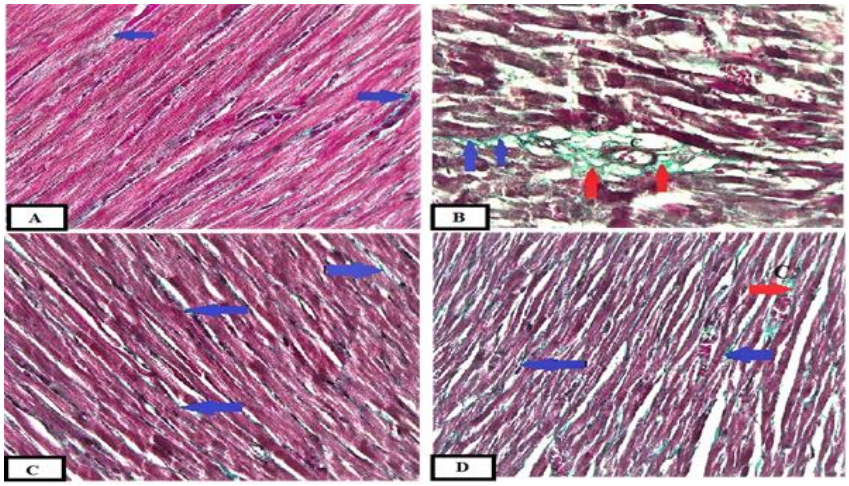

3. Electron microscope examination (Fig. 3):

The cylindrical myofibrils that make up the majority of the sarcoplasm in **(group I)** muscle fibers were clearly visible in histological sections. Ovate, central, and euchromatic best describe their nuclei. Numerous mitochondria were seen juxtanuclear and running in and beside myofibrils. The mitochondria were oval or round.

Two Z lines formed the boundaries of each sarcomere, which consisted of a center dark (A) band and two half of a light (I) band on the periphery. Myocytes had intercalated discs with a stepped shape. It was clear from ultrathin sections of **(group II)** that numerous myofibrils had been lysed, leading to an increase in the intermyofibrillar gap. The myofibrils of other cells were either very thin or exhibited signs of myofibril splitting. Most of the sarcomeres were shattered, the A and I bands merged, and the Z lines were disrupted.

Many mitochondria showed signs of total damage and degeneration at the same time as others showed signs of partial damage. Sarcolemma was disrupted.

Nuclei exhibited irregular and indented outlines. The ultrathin sections of muscle fibers in **(group III)** revealed lengthy, parallel arrays of cylindrical myofibrils filling the majority of the sarcoplasm. Ovate, central, and euchromatic best describe their nuclei. Numerous mitochondria were seen juxtanuclear and running in and beside myofibrils. The mitochondria were round or oval. Two Z lines delimited the boundaries of each sarcomere. Improvements were made to the ultrathin parts in **(group IV)**.

Myofibrils made up the bulk of the cellular material in the sarcoplasm. There were many thick and divided myofibrils, but many more that were cylindrical and consisted of longitudinal parallel arrays with tiny interfibrillar gaps. Their sarcomeres were improved; A and I bands were clearly seen and Z lines were intact. Mitochondria were partially improved, appeared oval or rounded and others were still damaged. Nuclei exhibited regular outlines

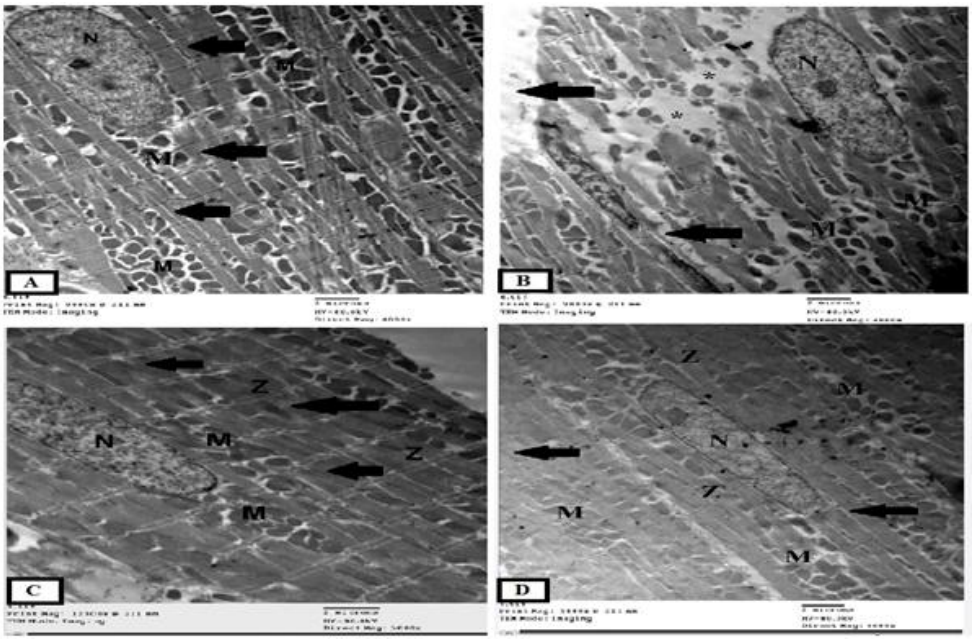

Table (1) Comparison between the studied groups regarding the mean area percent of collagen by Mallory's trichrome stain:

Items	Group 1	Group 2	Group 3	Group 4	P-value
Mean area percent	3.01±1.10	10.26±3.342	2.82±0.91	4.75±1.63	0.001*
	P1=0.002* P2=0.999 P3=0.686 P4=0.003* P5=0.013* P6=0.669				

P-value is significant

P1: Group 1 vs Group 2, P2: Group 1 vs Group 3, P3: Group 1 vs Group 4, P4: Group 2 vs Group 3, P5: Group 2 vs Group 4, and P6: Group 3 vs Group 4

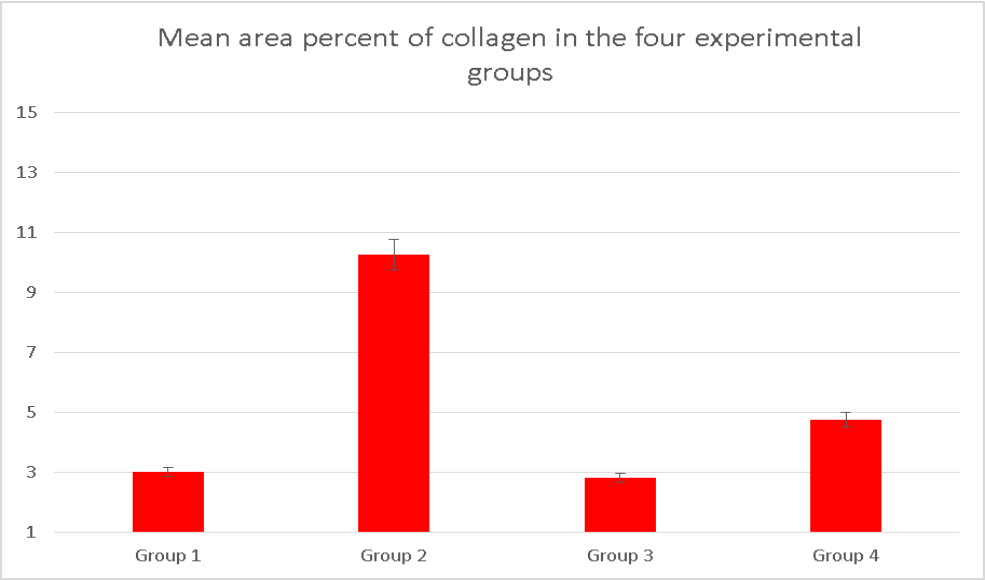

Histogram 1: Comparison between the four groups regarding the mean area percent of collagen fibers.

This table shows significantly increased mean area percent of collagen fibers in group 2 as compared to groups 1, 3 and 4. There was anon-significant difference when comparing Groups 1, 3 and 4.

4. Discussion:

Among the macrolide antibiotics, azithromycin is the most often used for treating bacterial respiratory tract infections. However, several studies have shown that the medication has a wide variety of pharmacological effects. Azithromycin is used to treat inflammatory illnesses including asthma and chronic obstructive lung disease due to its immunomodulatory effects (COPD). Furthermore, azithromycin may either directly or indirectly suppress viral load and replication by influencing the expression of antiviral genes (4).

The 2019 coronavirus disease outbreak (COVID-19) is officially a worldwide pandemic. The coronavirus 2 that causes severe acute respiratory distress syndrome is the culprit (SARS-CoV-2). Those already suffering from cardiovascular disease and who get COVID-19 tend to have more severe symptoms and die sooner as a result. In addition, individuals with COVID-19 have been documented to have low potassium levels, which may lead to electrocardiographic abnormalities such as a prolonged QT interval and might increase the risk of adverse responses with pharmacotherapies (17).

There are several medications being researched, with some even in the first stages of clinical trials. Chloroquine and Hydroxychloroquine (CQ/HCQ) alone or in combination with Azithromycin, Remdesivir, Lopinavir, and Interferon alpha-2b are among the most promising treatments available today (4). This study reviewed the potential cardiovascular risks associated with Azithromycin treatment.

Azithromycin induced cardiac oxidative stress, inflammation, and apoptosis in a rat model. As a result, there are alterations in the electrocardiogram, myocardial infarction, and mortality (11).

Whenever toxins, either naturally occurring or introduced artificially, reach a concentration at which they are harmful to the heart, this is called cardiotoxicity (18). Electrophysiological dysfunction or myocardial damage may result from cardiotoxicity. Additionally, mitochondrial dynamics is crucial in the development of neurological illnesses, suggesting that disturbances in mitochondrial dynamics may have deleterious consequences on cardiac cells (19).

Light microscopic examination of sections from control group **(group I)** showed normal architecture of cardiac muscles with striated branching cardiomyocytes, acidophilic cytoplasm, central oval vesicular nuclei, and intervening blood capillaries. Similar results reported by (20).

H & E-stained sections from Azithromycin group **(group II)** showed many areas of degeneration, myofibers disorganization, wide spaces in between myofibers, inflammatory infiltrate and cytoplasmic vacuoles due to its Oxidative stress (OS) which is considered a state of imbalance between oxidation and antioxidant effect in the body. It generates a slew of harmful byproducts, including reactive oxygen species (ROS), which have been linked to aging and other degenerative processes (21).

Disruption of the equilibrium between reactive oxygen species (ROS) and endogenous antioxidants (EAs) after damage may generate oxidative stress, which in turn can cause cardiotoxicity (22).

Cardiomyocytes with typical striated branching architecture, acidophilic cytoplasm, central oval vesicular nuclei, and interstitial blood capillaries were seen in H and E-stained sections from the Atorvastatin group **(group III)**. Similar results were reported by (23) who found that blocking Rac1 (a GTP-binding protein) driven ROS emission enhanced heart function in rats.

One of the classes of drugs known as statins, atorvastatin reduces cholesterol and other fats in the blood (10). With potent antioxidant and anti-inflammatory qualities, it helps keep heart disease healthy (24). In the current study, effects of Azithromycin on cardiac muscle of adult male albino rats and the possible protective role of Atorvastatin are histologically studied.

Sections from the Atorvastatin and Azithromycin group **(group IV)** demonstrated restoration of the arrangement of the heart muscle fibers compared to the Azithromycin group on light microscopic inspection, as shown by the present study's findings. Similar findings were made by (25).

Aside from decreasing cholesterol, atorvastatin has been demonstrated to have a wide variety of additional beneficial effects as ability to decrease ventricular mass, decrease inflammation, decrease ventricular fibrosis, alter metalloproteinase activity, decrease immune activation, increase arterial compliance, decrease thrombosis, and decrease oxidative stress that all can contribute to the prevention or attenuation of progressive ventricular remodeling in heart failure and improvement of ventricular function. These advantages are not shared by other cardioprotective medicines now used in

practice, indicating that statin treatment may play a unique and supplementary function in preventing cardiovascular disease (25).

Mallory's trichrome staining sections revealed low levels of collagen deposition between cardiomyocytes and surrounding blood vessels in **(group I)** and **(group III)** of the current investigation.

Myocardial fibrosis, as shown in rat heart sections, is caused by an accumulation of collagen fibers between cardiomyocytes and surrounding blood vessels, as seen in rats from **(group II)**. According to the explanations provided by (26), cardiac fibrosis caused by toxicity involves several elements and processes. Attenuation of matrix-degrading pathways and consequent excessive collagen buildup in the heart are main factors in this process. This is caused by a decrease in the proteolytic activity of "matrix metalloproteinases (MMPs) production by cardiac fibroblasts. Toxicity also plays a role by causing fibroblasts to change into myofibroblasts, the major effector cells in the fibrotic state, which increase collagen production. It has also been hypothesized that mitochondrial reactive oxygen species (ROS) generation and oxidative stress caused by toxicity play a significant role in cardiac fibrosis. Fibogenic effects of ROS have been observed. Fibrosis of the perivascular, endomysial, and perimysial spaces are the cumulative effects of all of these processes (26).

Collagen fibers were noticeably reduced in **(group IV)** rat tissue sections, while appearing almost normal in proximity to muscle fibers and capillaries. Current evidence suggests that Atorvastatin's antioxidant qualities are responsible for its significant hypolipidemic impact on heart muscle. It has been shown to scavenge free radicals before they may harm cells and produce cardiac fibrosis, as well as reduce reactive oxygen species (ROS) generation, oxidation of low-density lipoproteins, lipid peroxidation, and protein oxidation (24).

The present research confirms previous findings by showing a statistically significant difference between the four groups; specifically, group II showed a much higher collagen area than the other groups.

When comparing groups 1 and 3, groups 1 and 4, and groups 3 and 4, there was no statistically significant difference in the mean collagen area percent. The significance was between group 1 and 2, between group 2 and 3 and between group 2 and 4.

On ultra-structural inspection, the present research found that the sarcoplasm of control group **(group I)** rat muscle fibers was occupied by longitudinal parallel arrays of cylindrical myofibrils. Their nuclei were euchromatic and oval central. numerous

mitochondria were seen juxtanuclear and running in and beside myofibrils. The mitochondria were round or oval. Two Z lines formed the boundaries of each sarcomere, which consisted of a center dark (A) band and two half of a light (I) band on the periphery. Myocytes had intercalated discs. Similar results were reported by (20).

When compared to the other groups, the ultrathin sections of heart muscle from the rats in the Azithromycin group **(group II)** revealed the most significant damage and disruption of architecture. Many myofibrils were completely lysed, and the space between them expanded. The myofibrils of other cells were either very thin or exhibited signs of myofibril breaking. Sarcomeres were noticeably damaged, A and I bands were not distinguishable, and Z lines were disrupted in most regions. The nuclei had wavy and depressed outlines. Similar results were reported by (27). At the same time, the antioxidants in the mitochondria, such as superoxide dismutase (SOD) and glutathione (GSH), will rapidly degrade, resulting in decreased reactivity. This is because the interaction with the electron transport chain results in the uncoupling of electron transport from ATP production. Cardiovascular dysfunction occurs as a consequence of decreased mitochondrial antioxidant capability, because of the large concentration of mitochondria in myocardial tissue. In addition, ROS contributes to a variety of vascular disorders linked to the endothelial cell barrier's functional features (28).

The findings of the present investigation demonstrated that on ultra-structural analysis, the sarcoplasm of muscle fibers in the section from rats in **(group III)** was filled by longitudinal parallel arrays of cylindrical myofibrils. Ovate, central, and euchromatic best describe their nuclei. Juxtanuclear and positioned amid and parallel to myofibrils. Mitochondria were oval or rounded. Similar results were reported by (23) who observed that Atorvastatin improved cardiac function of rats via inhibiting Rac1 mediated ROS release.

When ultrathin sections of rats treated with Atorvastatin and Azithromycin **(group IV)** were analyzed, it was found that the sarcoplasm was mostly composed of myofibril. There were many thick and divided myofibrils, but many more that were cylindrical and consisted of longitudinal parallel arrays with tiny interfibrillar gaps. Some mitochondria were still damaged. Nuclei exhibited regular outlines. Similar results were reported by (29) who observed that Atorvastatin improved the cardiac function of rats after acute myocardial infarction through ERK1/2 (extracellular signal‐regulated kinase) pathway**.**

Indeed, the recent findings of clear and noteworthy improvement in the myocardium of Atorvastatin and azithromycin treated group **(group IV)** may provide highly encouraging insights for employing Atorvastatin to enhance cardiac function in rats following acute myocardial infarction.

5. Conclusion:

The present study concluded that Azithromycin administration induced remarkable damage of myocardium and disruption of myofibrils and sarcomeres and Atorvastatin administration induced restoration of the cardiac muscle fibers in histological and morphometric results.

6. Recommendations:

- Better to use Atorvastatin due to its cardio protective effect.
- Limit the usage of Azithromycin as an antibiotic due to its serious toxic effect on the heart..
- Further studies are required to uncover the exact toxic effect of Azithromycin on the heart.

Conflict of interest

No potential conflicts of interests exist.

Legend of Figures

Fig. 1: a photomicrograph of a longitudinal segment of the left ventricle, revealing **A (group I):** cardiac muscle fibers that are branching cylindrical with central vesicular oval nuclei (N) and acidophilic sarcoplasm (black arrow). The muscle fibers have tiny endomysial gaps (*). We saw fibroblasts with round nuclei (white arrows). A network of capillaries may be seen running in between muscle fibers (C). **B (group II):** Azithromycin rat tissue section demonstrating a lack of transverse striations in the cytoplasm of the majority of cells due to degeneration. Inflammatory cell infiltration marked enlargement of intercellular gaps (*) and congested, dilated blood capillaries (C). **C** (**Group III):** demonstrating the branching, cylindrical, nucleated, and acidophilic sarcoplasm of heart muscle fibers (black arrow). We saw fibroblasts with round nuclei (white arrows). **D (Group IV):** indicating seemingly normal cardiac muscle fibers. They have an acidophilic cytoplasm and a branching, cylindrical appearance (black arrows), with smaller than average intercellular gaps (*) White arrows point out fibroblasts. Nuclei of fibers are both vesicular and oval in shape (N). Congested blood capillaries are noticed (C). **(H&E stain × 400)**.

Fig. 2: A photomicrograph of longitudinal section of left ventricle of: **A (group 1**) showing minimal collagen fibers are deposited among myocytes (blue arrows).

B (group II): showing increased amount of collagen fibers deposition among muscle fibers (blue arrows) and around blood

capillaries (red arrows). **C (group III)** showing minimal collagen fibers deposition among muscle fibers (blue arrows).

D (group IV): showing moderate collagen fiber deposition around blood capillaries (red arrows) and minimal collagen fiber deposition among muscle fibers (blue arrows) **(Mallory's trichrome X400)**.

Fig. 3: In this electron micrograph of **A (group I)** cardiac muscle fibers, the sarcoplasm is dominated by parallel arrays of cylindrical myofibrils (black arrows). Myofibrils and the nucleus are surrounded by many mitochondria (M). Oval, euchromatic nucleus (N). Intermyofibrillar gaps are enlarged, and myofibrils are fragmented in **B (group II)** (black arrows). Numerous mitochondria have been destroyed, leaving behind just voids (*), while others have appeared abnormally (M). A depression marks the location of the nucleus (N). **C (Group III):** sarcoplasm dominated by parallel arrays of cylindrical myofibrils (black arrows) with intact Z lines (Z). Myofibrils and the nucleus are surrounded by many mitochondria (M). Oval, euchromatic nucleus (N). Most of the sarcoplasm is packed with myofibrils, as shown in **D (group IV).** Z lines are intact, and many myofibrils are cylindrical, arranged in longitudinal parallel arrays with small interfibrillar intervals (black arrow). The modified mitochondria have a more oval and rounded appearance (M). An ovoid, euchromatic nucleus **(X4000)**.

7. References:

1. Zimmermann P., Ziesenitz V.C., Curtis N., Ritz N. (2018): The immunomodulatory effects of macrolides—a systematic review of the underlying mechanisms. Front. Immunol. 9. 302.
2. Andreani J., Le Bideau M., Duflot I., Jardot P., Rolland C., Boxberger M. (2020): In vitro testing of combined hydroxychloroquine and azithromycin on SARS-CoV-2 shows synergistic effect. Microb. Pathog. 145.104228.
3. Du X., Zuo X., Meng F., Wu F., Zhao X., Li C. (2020): Combinatorial screening of a panel of FDA-approved drugs identifies several candidates with anti-Ebola activities. Biochem. Biophys. Res. Commun. 522. 862–868.
4. Gautret P, Lagier JC, Parola P, Hoang VT, Meddeb L, Mailhe M. (2020): Hydroxychloroquine and azithromycin as a treatment of COVID-19: results of an open-label non-randomized clinical trial. Int J Antimicrob Agents. 56. 105949 .
5. El-Shitany N.A., El-Desoky K. (2016): Protective effects of carvedilol and vitamin C against azithromycin-induced cardiotoxicity in rats via decreasing ROS, IL1-β, and TNF-α production and inhibiting NF-κB and caspase-3

expression. Oxidative Med. Cell. Longev. 2016:1874762.

6. Patel H., Calip G.S., DiDomenico R.J., Schumock G.T., Suda K.J., Lee T.A. (2019): Prevalence of cardiac risk factors in patients prescribed azithromycin before and after the 2012 FDA warning on the risk of potentially fatal heart rhythms. Pharmacotherapy: The Journal of Human Pharmacology and Drug Therapy. 40. 107–115.
7. Durrington PN, Mackness B, Mcknesss MI, (2011): Paraoxanase and atherosclerosis. Atheroscler Thromb Vasc Biol. 21. 473–480.
8. Bouitbir J, Charles AL, Echaniz-Laguna A, Kindo M, Daussin F, Auwerx J, Piquard F, Geny B, Zoll J. (2012): Opposite effects of statins on mitochondria of cardiac and skeletal muscles: A 'mitohormesis' mechanism involving reactive oxygen species and pgc-1 Eur Heart J . 33. 1397-1407.
9. Gao F, Ni Y, Luo Z, Liang Y, Yan Z, Xu X, Liu D, Wang J, Zhu S, Zhu Z. (2012): Atorvastatin attenuates tnf-alpha-induced increase of glucose oxidation through pgc-1alpha upregulation in cardiomyocytes. J Cardiovasc Pharmacol.59.500-506.
10. Mihaylova B, Emberson J, Blackwell L, Keech A, Simes J, Barnes EH, Voysey M, Gray A, Collins R, Baigent C. (2012): The effects of lowering ldl cholesterol with statin therapy in people at low risk of vascular disease: Meta- analysis of individual data from 27 randomised trials. Lancet. 380. 581-590.
11. Atli O., Ilgin S., Altuntas H., Burukoglu D. (2015): Evaluation of azithromycin induced cardiotoxicity in rats. Int. J. Clin. Exp. Med. 8. 3681–3690.
12. Kim Y.-H., Park S.-M., Kim M., Kim S.H., Lim S.-Y., Ahn J.-C. (2012): Cardioprotective effects of rosuvastatin and carvedilol on delayed cardiotoxicity of doxorubicin in rats. Toxicol. Mech. Methods. 22. 488–498.
13. Kiernan J K. (2001): Histological and Histochemical methods. In: Theory and practice. 3rd ed, London, New York, and New Delhy, Arnold Publisher.111-162 .
14. Bancroft JD, Layton C. (2013): The hematoxylin and eosin, connective and mesenchymal tissues with their stains. In: Suvarna SK, Layton C and Bancroft JD, editors. Bancroft's Theory and Practice of Histological Techniques. 7th edition, ch 10 and 11, Philadelphia, Churchill Living one. 173 – 212.
15. Woods AE, Stirling JW, (2013): Transmission electron microscopy applications. In: Suvarna SK, Layton C, Bancroft JD, editors. Theory and Practical Histological Techniques. 7th edition, ch 22, Philadelphia, Churchill Living one; 493 – 538.
16. Emsley R., Dunn G. and White I. (2010): Mediation and moderation of treatment effects in randomized controlled trials of

complex interventions. Stat Methods Med Res. 19(3). 237–270.

17. Ruan Q, Yang K, Wang W, Jiang L, Song J. (2020): Clinical predictors of mortality due to COVID-19 based on an analysis of data of 150 patients from Wuhan, China. Intensive Care Med. 46. 846–848.
18. Farías JG, Molina VM, Carrasco RA, Zepeda AB, Figueroa E, Letelier P. (2017): Antioxidant therapeutic strategies for cardiovascular conditions associated with oxidative stress. Nutrients. 9. 966.
19. Yosef T, Damri O, Agam G.(2019): Dual role of autophagy in diseases of the central nervous system. Front Cell Neurosci. 13. 196.
20. Dawood A and Hareedy H (2019): Differential effect of high fat diet (HFD) on the cardiac muscle of adult and aged female mice and the possible protective role of artichoke treatment: Histomorphometric and ultrastructural study. J Med Hist, Article 3, Volume 3, Issue 1, 36-54.
21. Paradies G, Paradies V, Ruggiero FM, Petrosillo G.(2018): Mitochondrial bioenergetics and cardiolipin alterations in myocardial ischemia-reperfusion injury: implications for pharmacological cardioprotection. Am J Physiol Heart Circ Physiol. 315. 1342.
22. Songbo M, Lang H, Xinyong C, Bin X, Ping Z, Liang S.(2019): Oxidative stress injury in doxorubicin-induced cardiotoxicity. Toxicol Lett. Vol: 307.Issue:48.
23. L.-P. An, S.-K. An, X.-H. Wei, S.-Y. Fu, H.-A. Wu. (2015): Atorvastatin improves cardiac function of rats with chronic cardiac failure via inhibiting Rac1/P47phox/P67phox-mediated ROS release. 20. 3940-3946.
24. Ramasubbu K, Estep J, White DL, Deswal A, Mann DL. (2008): Experimental and clinical basis for the use of statins in patients with ischemic and nonischemic cardiomyopathy. J Am Coll Cardiol .51. 415-426.
25. Sharma H., Pathan R.A., Kumar V., Javed S., Bhandari U. (2011): Anti-apoptotic potential of rosuvastatin pretreatment in murine model of cardiomyopathy. Int. J. Cardiol. 150. 193–200.
26. Anna B, Nikolas G. (2011): Aging and cardiac fibrosis. Aging and Disease. 2. 158-173.
27. Lin J, Lopez EF, Yufang Jin Y, Remmen HV, Bauch T, Han HC , Lindsey ML.(2008): Age-Related Cardiac Muscle Sarcopenia: Combining experimental and mathematical modeling to identify mechanisms. Exp Gerontol. 43(4). 296–306.
28. Datta S, Cano M, Ebrahimi K, Wang L, Handa JT.(2017): The impact of oxidative stress and inflammation on

RPE degeneration in non-neovascular AMD. Prog Retin Eye Res. 60. 218.

29. Zeng H.-T, Zhao M, Zhang Z.-X, Liu Z.-L, , Zhong S.-M. (2019): Atorvastatin improves the cardiac function of rats after acute myocardial infarction through ERK1/2 pathway. 23(16):7120-7127.